POLISH MARITIME RESEARCH Special Issue 2017 S2 (94) 2017 Vol. 24; pp. 111-117
10.1515/pomr-2017-0072

AN ANALYTICAL SOLUTION FOR DYNAMIC RESPONSE OF WATER BARRIER SUBJECTED TO STRONG SHOCK WAVES CAUSED BY AN UNDERWATER EXPLOSION TO DAMS

Lu Lu[1,2,3*], A.Prof. Dr.,
Degao Zou[2], Prof. Dr.,
Ye Zhu[2,3*], Dr.,
Yun Dong[3], Prof. Dr.,
Chunyuan Zuo[1], Dr.,
YachaoWu[1], La. M.S.

[1] Faculty of Management Engineering, Huaiyin Institute of Technology, Huai'an 223003, China
[2] The State Key Laboratory of Coastal and Offshore Engineering, Dalian University of Technology, Dalian, 110623, China
[3] Faculty of Architecture and Civil Engineering, Huaiyin Institute of Technology, Huai'an 223001, China
* Corresponding author

ABSTRACT

Shock waves arriving at a dam site are close to plane waves when the center of an underwater explosion is far from the dam site. In general, the wave pressure is calculated with COLE empirical formula. The COLE formula is a negative exponential function with respect to time. In this paper, a new analytical solution algorithm is proposed, which does not require the use of step-by-step time integration. In Comparison with the step-by-step time integration, the proposed algorithm requires relatively less calculation and avoids high-frequency oscillation. Furthermore, the vertical upstream surface and the sloping upstream surface in two types of the dams are analyzed in this paper. The research results indicate that the analytical solution can be applied for a dam with a vertical upstream surface. However, because the upstream face of a dam is inclined, the analytical solution can be obtained only for dams that are at lower height. Whenever the height of a dam is higher, then no analytical solution can be obtained, and only the use of step-by-step time integration can obtain a solution.

Keywords: Underwater explosion, Shock wave, Dam, Analytical solution, Dynamic response

INTRODUCTION

Although a high dam subjected to a strong underwater shock wave is of small probability, to ensure the safety of lives and property, this research topic has attracted the attention of research and management personnel for a long time. Two of the most common approaches used in this research field are "numerical simulation" and "physical simulation". Wang et al.[1] foun state that a submerged explosion causes significantly more damage to a dam in the water rather than the same mass of explosion in the air via the numerical study. Hence, more attention should be paid to the shock wave from an underwater explosion and the subsequent response of the dam structures. Model dam tests using different impact loads were conducted by Lu et al. [2,3,4,5]. The results show that when the shock wave pressure of a 150 m high concrete gravity dam upstream reaches nearly to 4.0 MPa, then the dam head has been broken.

Many studies have in-depth analyses of the responses of dams during strong earthquakes. Wang et al.[6] successfully numerically simulate the damage phenomenon of the Koyna gravity dam subjected to earthquake, and apply the elastoplastic damage model to analyze the damage-cracking behavior of arch dams. Xu et al. [7] studied about the concrete slab damage under earthquake load and the development process using a concrete plastic-damage model[8], in which the damage variable can clearly determine the damage distribution and areas of weakness in the slabs. Although this paper belongs to the set of papers involving the dynamic analysis, it is different from studies of the dynamic response of the dam to a seismic load. Firstly, the duration of a strong shock wave from an underwater explosion is short, usually measured in microseconds, and the duration of an earthquake is much longer. Secondly, the shock wave of an underwater explosion can occur directly on the dam's upstream surface, while a seismic wave comes from the valley foundation, and the dam body's movement is caused by hydrodynamic pressure.

Besides that, many scholars have studied the dynamic responses of concrete and composite structures under explosive load in the air. Tai et al. [9] numerically simulated the dynamic response of a reinforced concrete slab subjected to air blast loads. Thiagarajan et al.[10] conducted the tests and finite element analysis of doubly reinforced concrete slabs subjected to blast loads. Chen et al. [11] simulated a prestressed reinforced concrete beam subjected to blast loading. Liu et al. [12] examined the simplified blast-load effects on the columns and bent beams of highway bridges. In these various numerical studies, the step-by-step time integration method is commonly used. The shock wave arriving at the dam site is close to a plane wave in character when the center of the underwater explosion is far from the dam site. Thus, the wave pressure is often calculated using the COLE empirical formula. The COLE empirical formula[13] is a negative exponential function with respect to time. In this paper, one analytical solution algorithm is given with no application of step-by-step time integration. Moreover, by comparison to the previous numerical studies, there is limited calculation involved in this study to avoid high-frequency oscillation. Generally, this paper presents one new simplified research approach.

THE VERTICAL UPSTREAM SURFACE OF A DAM

The diagram of the vertical upstream surface of a dam (i.e., gravity dam) subjected to a strong shock wave is shown in Fig. 1.

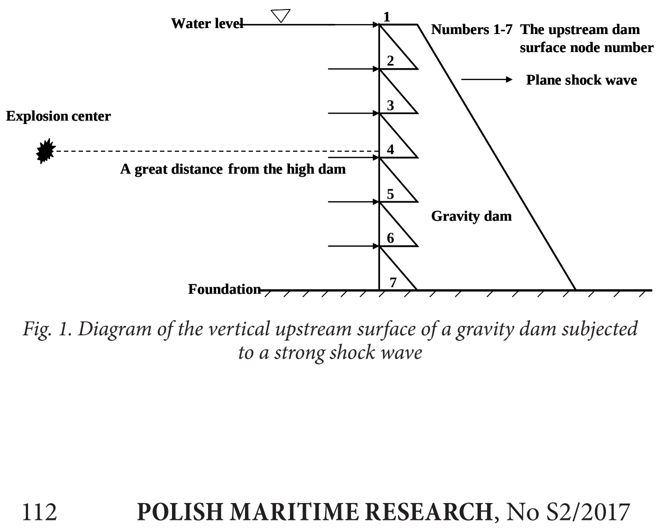

Fig. 1. Diagram of the vertical upstream surface of a gravity dam subjected to a strong shock wave

After spatial discretization, the vibration equation of the dam body is represented by a matrixas follows:

$$[M]\{\ddot{u}\}+[C]\{\dot{u}\}+[K]\{u\}=\{R\}p_d(t) \quad (1)$$

where $[M]$ is the mass matrix, $[C]$ is the damping matrix, and $[K]$ is the stiffness matrix. $[\ddot{u}]$, $[\dot{u}]$, and $[u]$ are the acceleration, velocity, and displacement vector of the nodes, respectively. $\{R\}$ is the distribution of the shock wave function vector, and $p_d(t)$ isthe pressure on the surface of the dam.

The pressure of a shock wave, which is a function of time, at a given position in water is $p_w(t)$; it abruptly increases to $(P_w)_{\max}$ when an explosion is initiated (an event with a duration of less than 10^{-7} s), followed by an exponential reduction. The Cole empirical formula yields

$$p_w(t)=(P_w)_{\max}e^{-\theta \cdot t} \quad (2)$$

where $P_{\max}$ is the maximum pressure of the shock front at a certain position, θ is the time coefficient, and T is the duration before the arrival of the shock wave. The relationship between $P_{\max}$ and θ is

$$P_{max}=K_1(\sqrt[3]{W}/R)^{A_1}\ (\text{MPa}) \quad (3)$$

$$\theta=\frac{1}{K_2W^{1/3}}\left(\frac{R}{\sqrt[3]{W}}\right)^{A_2}\times 10^4\ (1/\text{s}) \quad (4)$$

where R is the distance from the origin of the explosion to the point at which measurements are made (in meters); W is the amount of explosives (in kg); and the coefficients A_1, A_2, K_1, and K_2 are constants that depend on the types of explosive.

Once the shock wave comes into contact with the structure, the wave is reflected and transmitted to the structure. Smith and Hetherington[14] solved the equilibrium and compatibility equations at the interface between two different materials (graphically shown in Figure 2), to determine the resultant interface stresses:

$$\sigma_b=2\left(\frac{\sqrt{E_2\rho_2}}{\sqrt{E_1\rho_1}+\sqrt{E_2\rho_2}}\right)\sigma_a=2\left(\frac{\rho_2\sqrt{\frac{E_2}{\rho_2}}}{\rho_1\sqrt{\frac{E_1}{\rho_1}}+\rho_2\sqrt{\frac{E_2}{\rho_2}}}\right)\sigma_a \quad (5)$$

where Equation (5) describes the relationship between an incident wave σ_a and a transmitted wave σ_b. Each material is defined by a Young's modulus, E, and a density, ρ. In Fig. 2., σ_r is the reflected wave.

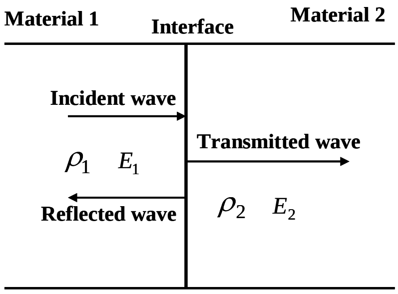

Fig.2. Diagram of the vertical upstream surface of a gravity dam subjected to a strong shock wave

If material 2 is conventional concrete, then $E_2 \approx 2.2\times10^{10} N/m^2$ and $\rho_2 \approx 2400kg/m^3$. If material 1 is water, then the wave velocity of the water is $\sqrt{\frac{E_1}{\rho_1}} \approx 1400m/s$.

Substituting the related parameters into Equation (5), we obtain $\sigma_b = 1.76\sigma_a$, which implies that regardless of the pressure generated by the underwater explosion, approximately twice that amount of pressure is transmitted to the concrete structure. Thus, for this study, we define

$$(P_d)_{\max} = 2P_{\max} \tag{6}$$

$$p_d(t) = 2p_w(t) \tag{7}$$

Because $p_d(t)$ is a negative exponential function, we have the following:

$$\left.\begin{aligned}\{u(t)\} &= \{u\}e^{-\theta t}\\ \{\dot{u}(t)\} &= -\theta\{u\}e^{-\theta t}\\ \{\ddot{u}(t)\} &= \theta^2\{u\}e^{-\theta t}\end{aligned}\right\} \tag{8}$$

where $\{u\}$ is a vector with no time variable t. Substituting Equations (7) and (2) into Equation (1) gives

$$\left(\theta^2[M] - \theta[C] + [K]\right)\{u\} = \{R\}2P_{\max} \tag{9}$$

According to Rayleigh damping, the damping matrix is given by

$$[C] = \alpha_1[M] + \alpha_2[K] \tag{10}$$

where α_1 and α_2 are expressed as

$$\alpha_1 = \frac{2\xi_1\omega_1\omega_2}{\omega_1 + \omega_2} \tag{11}$$

$$\alpha_2 = \frac{2\xi_2}{\omega_1 + \omega_2} \tag{12}$$

where ω_1 and ω_2 are the predominant natural frequencies of the structure. For gravity dams, the first and the second eigenfrequency of the gravity dam are preferred. ξ_1 and ξ_2 are the natural damping ratios for ω_1 and ω_2, respectively; take $\xi_1 = \xi_2 = 0.05$. Substituting Equation (10) into Equation (9) gives

$$\left\{\left(\theta^2 - \alpha_1\theta\right)[M] + \left(1 - \theta\alpha_2\right)[K]\right\}\{u\} = \{R\}2P_{\max} \tag{13}$$

Because the impact wave pressure $p_d(t)$ acts on only the nodes of the upstream dam surface, the R vector of N dimension can be divided into two sub-vectors. Let

$$\left.\begin{aligned}\{R_1\}_i &= \{1\}\\ \{R_2\}_{N-i} &= \{0\}\end{aligned}\right\} \tag{14}$$

where the subscripts i and $N-i$ denote the dimensions of the vector or matrix. Let

$$[W] = \left(\theta^2 - \alpha_1\theta\right)[M] + \left(1 - \theta\alpha_2\right)[K] \tag{15}$$

Equation (13) can be abbreviated as

$$[W]\{u\} = \begin{Bmatrix}R_1\\R_2\end{Bmatrix}2P_{\max} \tag{16}$$

$[W]$ and $[u]$ reference the $[R]$ form and are written in block form as follows:

$$\left.\begin{aligned}[W] &= \begin{bmatrix}(W_{11})_{i\times i} & (W_{12})_{i\times(N-i)}\\ (W_{12})_{(N-i)\times i} & (W_{22})_{(N-i)\times(N-i)}\end{bmatrix}\\ \{u\} &= \begin{Bmatrix}(u_1)_i\\ (u_2)_{N-i}\end{Bmatrix}\end{aligned}\right\} \tag{17}$$

Equation (16) can be rewritten as follows:

$$\begin{bmatrix}W_{11} & W_{12}\\ W_{21} & W_{22}\end{bmatrix}\begin{Bmatrix}u_1\\u_2\end{Bmatrix} = \begin{Bmatrix}1\\0\end{Bmatrix}2P_{\max} \tag{18}$$

Reorganizing the above equation yields

$$\left.\begin{aligned}[W_{11}]_{i\times i}\{u\}_i + [W_{12}]_{i\times(N-i)}\{u\}_i &= \{1\}_i 2P_{\max}\\ [W_{21}]_{(N-i)\times i}\{u\}_{N-i} + [W_{22}]_{(N-i)\times(N-i)}\{u\}_{N-i} &= \{0\}_{N-i}\end{aligned}\right\} \tag{19}$$

By the second equation in Equation (19), the equation (20) can be obtained.

$$\{u_2\} = -[W_2]^{-1}[W_2]\{u_1\} \quad (20)$$

Substituting Equation (20) into the first equation in Equation (19), $([W_{11}]\{u_1\} - [W_{12}][W_{22}]^{-1}[W_{21}]) = \{1\}2P_{\max}$ is deduced. By collating the above equation, we can express

$$([W_{11}]_{i\times i} - [W_{12}]_{i\times(N-i)}[W_{22}]^{-1}{}_{(N-i)\times(N-i)}[W_{21}]_{(N-i)\times i})\{u_1\}_i = \{1\}_i 2P_{\max} \quad (21)$$

Solving the algebraic equation (21) yields $\{u_1\}_i$. Because the number of nodes is not high in the dam upstream surface, as long as a low-dimensional algebra equation can obtain an analytical solution $\{u_1\}_i$. Next, formula (20) is used to obtain $\{u_2\}_{N-i}$. Equation (8) can be used to calculate the change of the displacement, velocity and acceleration vs. time. Solving $[W_{22}]^{-1}$ represents the largest part of the computing workload, which is a very small computing workload compared with that of the step-by-step time integration method.

SLOPING UPSTREAM SURFACE OF THE CONCRETE-FACED ROCKFILL DAM

The upstream face of a concrete-faced rockfill dam is inclined; thus, the shock wave arrived at the dam site is shown in Fig. 3.

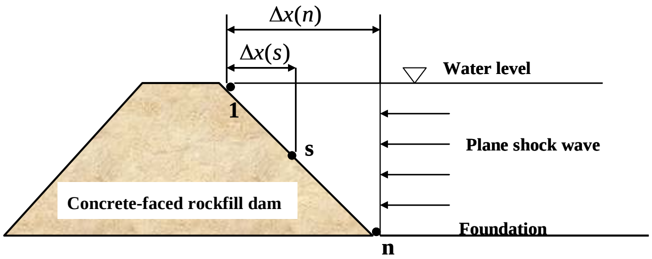

Fig. 3. Diagram of the sloping upstream surface of a concrete-faced rockfill dam subjected to a strong shock wave

When the shock wave arrives in node *n*, the other nodes on the dam are not subjected to the shock wave. If the shock wave reaches 1 node, at which point the time is zero ($t = 0$), then the pressure expression of 1 node is $p(1) = 2P_{\max 1}e^{-\theta t}$. SubstitutingEquations (3) and (4) into $p(1) = 2P_{\max 1}e^{-\theta t}$ gives

$$p(1) = 2k_1(\sqrt[3]{W}/R)^{k_2} e^{-\left(\frac{R}{\sqrt[3]{W}}\right)^{k_4}(K_3\sqrt[3]{W})^{-1}\times t} \quad (22)$$

The pressure expression of the S node is

$$p(S) = 2k_1(\sqrt[3]{W}/(R+\Delta x(s)))^{k_2} e^{-\left(\frac{R+\Delta x(s)}{\sqrt[3]{W}}\right)^{k_4}(K_3\sqrt[3]{W})^{-1}\times\left(t+\frac{\Delta x(s)}{C}\right)} \quad (23)$$

where *C* is the velocity of sound in water, $\Delta x(s)$ is the horizontal distance between the S node and 1 node, and $\frac{\Delta x(s)}{C}$ is the time interval between the shock wave to reach the S node and 1 node. When the upstream face of the dam is inclined, the analytical solution of the time given in this paper cannot be used and the step-by-step time integration is required. However, assuming that the dam is not high and the C value is large, the initial period can be omitted ($t = 0$ before) and we still obtain the analytic solution after time t. The distribution function $\{R\}$

is not $\begin{Bmatrix} 1 \\ - \\ 0 \end{Bmatrix}$, but rewritten as $\begin{Bmatrix} 1 \\ \vdots \\ e^{-\theta\frac{\Delta x(i)}{C}} \\ - \\ 0 \\ 0 \\ 0 \end{Bmatrix}$.

CALCULATION EXAMPLE ANALYSIS

A gravity dam with a vertical upstream surface can be discussed as an example. In this example, we consider an analysis of the Koyna dam, which is located in the southwest of India, Karnataka Province. The geometry of a typical non-overflow monolith of the Koyna dam is illustrated in Fig. 4(a). The monolith is 103 m high and 71 m wide at its base. The upstream wall of the monolith is assumed to be straight and vertical, which is slightly different from the real configuration. The depth of the reservoir is 103 m in this study. Following the work of other investigators[8], we consider a two-dimensional analysis of the non-overflow monolith assuming plane stress conditions. The spatial discrete grid used for the analysis is shown in Fig. 4(b). In Fig. 4(b), 1# and 2# are our observation points.

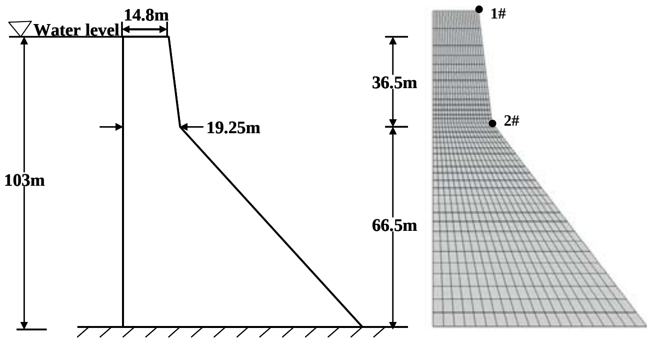

(a) the Koyna dam *(b) the spatial discretization grid of the dam*

Fig. 4. Dimensions of the Koyna dam and the spatial discretization grid

The mechanical behavior of the concrete material is modeled using the linear elastic model. According to the available design information, the following properties were used in the analysis: density = 2643 kg/m^3, modulus of elasticity = 31027 MPa, and Poisson's ratio = 0.15. In this study, the damping ratio for the concrete dam was assumed to be 5% in the dynamic analysis.From a natural frequency extraction analysis of the dam, the first and second eigenfrequency are found to be ω_1=18.861 rad/s and ω_2=49.973 rad/s, respectively. We use the equations (11) and (12) to obtain $\alpha_1 = 0.8216$ and α_2-8.7166e-04, respectively.

For this research, prior to shock loading, the dam was subjected to static loading, including self-weight and hydrostatic pressure. The dam being subjected to static loading is assumed as the initial state. The charge used for the analysis was 10000 kg of TNT. The values of the coefficients A_1, A_2, K_1, and K_2 for an underwater TNT explosion are $A_1 = 1.180$, $A_2 = -0.185$, $K_1 = 52.12$ and $K_2 = 0.0895$, respectively[15]. The distance from the origin of the explosion to the dam site is $R = 500$ m. The shock wave was determined from the Cole empirical formula, of which the peak pressure was $P_{\max} = 1.2751$ MPa and the recording duration was 24.1489 ms, as shown in Fig.5.

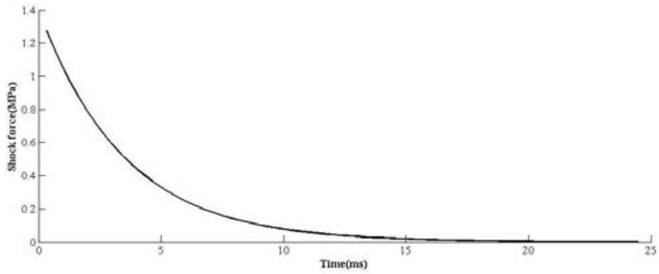

Fig. 5. Time history graphs of the shock wave loading

Here, the two methods used in the calculations were analyzed. One method uses the accurate time-dependent solution algorithm presented earlier in this paper. The other method uses the central difference rule to perform the integral of the motion equation in time domain (it is a form of step-by-step time integration).

1) The accurate solution of the time-dependent algorithm

The maximum pressure of the shock wave is $P_{\max} = 1.2751$ MPa; from equation (5), the maximum shock force acting on upstream surface is $(P_d)_{\max} = 2.5502$ MPa. After calculation, the horizontal x-axis displacement of the 1# points and 2# points is 0.243063 m and 0.0886145 m, respectively. By the first equation in Equation (8), the change of the displacement can be obtained in the time domain.

2) The explicit central-difference integration rule to perform the integral of the motion equation in the time domain

Jin andDing [16] demonstrated that Abaqus/Explicit can be used to predict the transient response of ship structures that experience loading by an acoustic pressure shock wave resulting from an underwater explosion (UNDEX). In this paper, although the focus of research is not the underwater explosion and shock wave propagation characteristics because of the similarity between the shock wave and the dam-water system considered here, Abaqus/Explicit was chosen as the numerical analysis platform. When the acoustic fluid behavior is linear (i.e., no cavitation), the total acoustic pressure within the fluid consists of an incident wave and a scattered wave component. A finite element model of the dam-water system was adopted. The dam base was completely constrained. A CPS4R element was adopted to simulate all parts of the dam. The external fluid was meshed with AC3D4 acoustic tetrahedral elements. The water density is 10 kN/m^3, the bulk modulus is 2140 MPa, and the speed of sound in water is 1400 m/s. The acoustic structural coupling between the fluid mesh acoustic pressures and the dam structural displacements at their common surfaces (the wetted interface) was accomplished with the *TIE constraint option in Abaqus. The dam two-dimensional finite element model is shown in Fig.6.

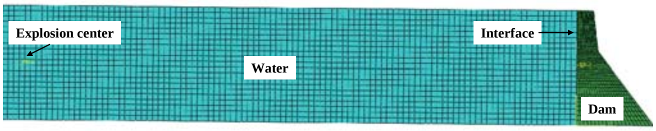

Fig. 6. Finite element mesh of the dam and water

By the above two methods, the horizontal displacement changes of 1# point and 2# point along with the time are shown in Fig. 7.

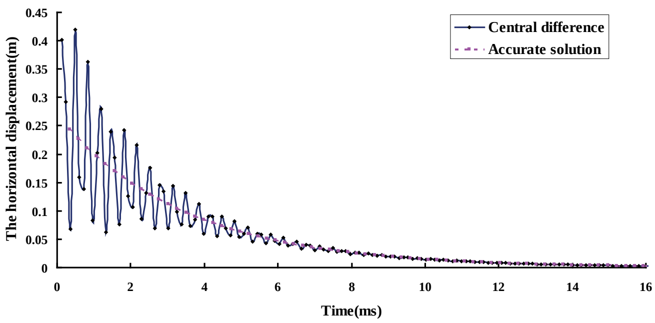

(a) 1# point

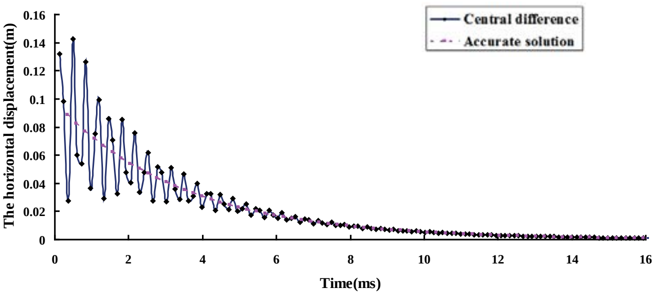

(b) 2# point

Fig. 7. The horizontal displacement history of the dam: (a) 1# point; (b) 2# point

The equations of motion for the body are integrated using the explicit central-difference integration rule in this study.

$$\begin{cases} \dot{u}_{i+2}^{N} = \dot{u}_{i-\frac{1}{2}}^{N} + \dfrac{\Delta t_{i+1} + \Delta t_i}{2} \ddot{u}_i^N \\ u_{i+1}^{N} = u_i^N + \Delta t_{i+1} \dot{u}_{i+\frac{1}{2}}^{N} \end{cases} \quad (24)$$

where N is a degree of freedom. $\ddot{u}$, $\dot{u}$, and u are the acceleration, velocity, and displacement, respectively. The subscript i refers to the increment number in an explicit dynamics step, and $i-\frac{1}{2}$ and $i+\frac{1}{2}$ refer to the midincrement values. The central difference integration operator is explicit as the kinematic state can be advanced using known values of $\dot{u}_{i-\frac{1}{2}}^{N}$ and $\ddot{u}_i^N$ from the previous increment. The explicit integration rule is quite simple but by itself does not provide the computational efficiency associated with the explicit dynamics procedure. The key to the computational efficiency of the explicit procedure is the use of diagonal element mass matrices because the accelerations are at the beginning of the increment. The explicit procedure of integration through time is based on many small time increments. The central difference operator is conditionally stable, and the stability limit for the operator is given in terms of the highest eigenvalue in the system. In Abaqus/Explicit, a small amount of damping is introduced to control high-frequency oscillations. With damping, the stable time increment is given by

$$\Delta t \le \frac{2}{\omega_{\max}}(\sqrt{1+\xi_{\max}} - \xi_{\max}) \quad (25)$$

where $\xi_{\max}$ is the fraction of critical damping in the highest mode. Contrary to our usual engineering intuition, introducing damping to the solution reduces the stable time increment. The time-increment based scheme in Abaqus/Explicit is fully automatic and requires no user intervention. The maximum frequency of the model is related to many factors. Abaqus/Explicit initially uses the element by element estimates. As the step proceeds, the stability limit will be determined from the global estimator once the algorithm determines that the accuracy of the global estimation is acceptable. Thus, the high-frequency oscillation phenomenon is difficult to avoid for the numerical analysis of a high dam subjected to strong shock waves caused by an underwater explosion using the explicit central-difference integration rule. High-frequency oscillation can cause serious distortion. Additionally, the well-known Wilson-θ integral method[17,18] is characterized by unconditionally stable convergence but has reduced the calculation accuracy.

CONCLUSIONS

In this paper, the shock wave to dam site is similar to the plane wave when the center of the underwater explosion is far from the dam site. The wave pressure is calculated based on the COLE empirical formula which is a negative exponential function with respect to time. Relative to the time dependence, a new analytical solution is proposed in this paper that does not require the use of step-by-step time integration. The following conclusions can be drawn based on the analysis results.

1) The analytical solution algorithm can be obtained for a dam (i.e., gravity dam) with a vertical upstream surface. However, when the upstream surface of a dam is inclined (i.e., concrete-faced rockfill dam), then the shock wave does not arrive at the upstream surface of a dam at the same time. Thus, the time-dependent analytical solution algorithm cannot be used and step-by-step time integration is required. However, if the dam is not high and the C value is large, the initial period can be omitted ($t = 0$ before) and the analytical solution after time t can be used. The distribution functions must be rewritten in this case.
2) In this paper, we also consider an analysis of the Koyna dam. Abaqus/Explicit was chosen as the numerical analysis platform. The results state that the high oscillation phenomenon is difficult to avoid for the numerical analysis of a high dam subjected to strong shock waves caused by an underwater explosion using the explicit central-difference integration rule. High-frequency oscillation can cause serious distortion.
3) In this paper, we provide the analytical solution algorithm to calculate the same case. The results indicate that the proposed approach is not only capable to improve the calculation efficiency but also completely eliminate the high-frequency oscillation phenomenon.

On the basis of this study, the nonlinear dynamic analysis of a dam subjected to strong shock waves caused by an underwater explosion can be further studied.

ACKNOWLEDGEMENTS

This work was supported by the [the Natural Science Foundation of China] under Grant [No. 51379028], [the research Funds of the State Key Laboratory of Structural Analysis for Industrial Equipment of Dalian University of Technology] under Grant [No. GZ1409], and the State Key Laboratory of Coastal and Offshore Engineering of China (Grant No. LP1714).

REFERENCES

1. G.Wang, S.Zhang, Y.Kong and H.Li. Comparative Study of the Dynamic Response of Concrete Gravity Dams Subjected to Underwater and Air Explosions. Journal of Performance of Constructed Facilities, 04014092, 2014.

2. Lu L, Li X, Zhou J. Protection Scheme for Concrete Gravity Dam Acting by Strong Underwater Shock Wave. Advanced Science Letters, Adv. Sci. Lett. Vol. 19, No. 1, pp. 238-243,2013.

3. L.Lu, X.Li and J.Zhou. Study of damage to a high concrete dam subjected to underwater shock waves. Earthquake Engineering and Engineering Vibration, vol.13, no.2, pp.337-346, 2014.

4. Lu L, Li X, Zhou J, et al. Numerical Simulation of Shock Response and Dynamic Fracture of a Concrete Dam Subjected to Impact Load. Earth Sciences Research Journal, vol.20, no.1,pp.1-6, 2016.

5. Lu Lu, Xianjing Kong, Yun Dong, et al. Similarity Relationship for Brittle Failure Dynamic Model Experiment and Its Application to a Concrete Dam Subjected to Explosive Load. Int. J. Geomech, 04017027,2017.

6. J. T.Wang, D. D. Lv, F.Jin and C. H.Zhang. Earthquake damage analysis of arch dams considering dam–water–foundation interaction. Soil Dynamics and Earthquake Engineering,vol. 49, pp.64-74, 2013.

7. B.Xu, D.Zou, X.Kong, Z.Hu and Y.Zhou. Dynamic damage evaluation on the slabs of the concrete faced rockfill dam with the plastic-damage model. Computers and Geotechnics, vol.65, pp.258-265, 2015.

8. J.Lee and G. L.Fenves. A plastic‐damage concrete model for earthquake analysis of dams. Earthquake engineering & structural dynamics, vol.27, no.9, pp. 937-956, 1998.

9. Y. S.Tai, T. L.Chu, H. T.Hu and J. Y.Wu. Dynamic response of a reinforced concrete slab subjected to air blast load. Theoretical and applied fracture mechanics, vol.56, no.3, pp.140-147, 2011.

10. G.Thiagarajan, A. V. Kadambi , S.Robert and C. F.Johnson. Experimental and finite element analysis of doubly reinforced concrete slabs subjected to blast loads. International Journal of Impact Engineering, vol.75, pp.162-173, 2015.

11. W.Chen, H.Hao and S.Chen. Numerical analysis of prestressed reinforced concrete beam subjected to blast loading. Materials & Design, vol.65, pp.662-674,2015.

12. H.Liu, D. M.Torres, A. K.Agrawal , Z.Yi and G.Liu. Simplified Blast-Load Effects on the Column and Bent Beam of Highway Bridges. Journal of Bridge Engineering. ASCE, published online, 2015.

13. R.H. Cole and R.Weller. Underwater explosions. Princeton: Princeton University Press, 1948.

14. P. D.Smith and J. G.Hetherington. Blast and ballistic loading of structures. Digital Press, 1994.

15. C. C.Liang and Y. S. Tai. Shock responses of a surface ship subjected to noncontact underwater explosions. Ocean Engineering, vol.33, pp.5, pp.748-772, 2006.

16. J.Qiankun and D. Gangyi. A finite element analysis of ship sections subjected to underwater explosion. International Journal of Impact Engineering, vol.38, pp.7, 558-566, 2011.

17. M.Shimada, S.Masuri and K. K.Tamma. A novel design of an isochronous integration [iIntegration] framework for first/second order multidisciplinary transient systems. International Journal for Numerical Methods in Engineering, vol.102, no.(3-4), pp.867-891, 2015.

18. L.Zhang, T.Liu and Q. Li. A Robust and Efficient Composite Time Integration Algorithm for Nonlinear Structural Dynamic Analysis. Mathematical Problems in Engineering, published online, 2015.

CONTACT WITH THE AUTHOR

Lu Lu

e-mail: llzhxy@aliyun.com
tel.: 0086+15161753545

Faculty of Management Engineering
Huaiyin Institute of Technology
Huai'an Jiangsu, 223003
China